

Using SAR Satellite Imagery for Potential Green Roof Retrofitting for Flood Mitigation in Urban Environment

Mirka Mobilia^a and Antonia Longobardi^b

Department of Civil Engineering, University of Salerno, Via Giovanni Paolo II, 132, Fisciano (SA), Italy


Keywords: Green Roof, SAR Images, SWMM, Sarno River Basin.


Abstract: Green roofs (GRs) represent a valid tool to mitigate the negative effects of urban floods. The aim of the present work is to test the hydrological behaviour of GRs at basin scale using Storm Water Management Model (SWMM), with an application to Preturo municipality located within the Sarno river basin (southern Italy) which during the last two decades was interested by the occurrence of many hazardous flash floods. The analysis of two sets of satellite images acquired between 1995 and 2016 by SAR sensors, showed a correlation between the increase of soil sealing and the occurrences of urban flooding during the same period. This finding suggests that the GR extensive adoption could contribute to a successful stormwater management. The suitability for GR retrofit depends on a number of criteria. In Preturo municipality, the fulfilment of these criteria was investigated using satellite images from Google Earth. The GRs retrofit potential of the studied area amounts to 7% of the total surface. The hydrological behaviour of the GR retrofit scenario was compared to the reference one which considers the actual land cover. The GR scenario better performs than the traditional one with a reduction of the runoff volume and peak flow of respectively 3.5% and 18.9% and an increase of the delay time of 8.2%.

1 INTRODUCTION

The most direct impact of the rapid population growth is the demand for new buildings, which causes the increase of urban areas all over the world. The uncontrolled soil sealing leads to increasingly severe and frequent urban flooding events (Mobilia et al., 2015, Longobardi et al., 2016, Khramtsova et al. 2020). The low impact development (LID) strategies consist of a number of practices, which mimic the site's predevelopment hydrologic functions so as to mitigate the hazardous hydrological events (Chui et al., 2016). Among these, the green roofs (GR) are better able to minimize, detain and retain the extra-runoff (Sartor et al., 2018, Longobardi et al., 2019, Mobilia et al., 2017). Over the years, modelling results have confirmed the role of GRs in restoring the natural water regime by reducing the runoff production. Some of the approaches used in previous studies to reproduce the GRs hydrological behavior, involved the use of water balance model (Starry et al., 2016, Mobilia and Longobardi, 2020a, Mobilia and Longobardi, 2017), NASH cascade model

(Krasnogorskaya et al., 2019), Hydrus model (Mobilia and Longobardi, 2020b) and the rainfall-runoff simulation model by Environmental Protection Agency (EPA), SWMM (Storm Water Management Model) (Haowen et al. 2020). In particular, the last one has proved to be very accurate and user-friendly (Wanniarachchi, 2012). Several studies concerning GR hydrological modelling at basin scale have demonstrated that, if widely implemented, these tools allow to significantly reduce the negative impact of urban flooding by decreasing the runoff volume even up to 25% and the peak discharge to 36% (Versini et al., 2015). Unfortunately, the extensive adoption of vegetated cover in an urban basin is prevented by some barriers, indeed, several criteria should be considered when determining whether a roof is suitable for retrofitting including the roof slope, number of stories, orientation of the roof, number of site boundaries (Wilkinson and Reed, 2009). In this context, satellite imagery could be used to identify the buildings with the potential for GR retrofit. The present research aims at investigating the ability of GRs, at large scale, to reduce the hydraulic load on

^a  <https://orcid.org/0000-0001-7018-3592>

^b  <https://orcid.org/0000-0002-1575-0782>

urban drainage system in order to mitigate urban flooding events. Two scenarios have been simulated, using SWMM and compared in terms of runoff volume, peak flow and delay time during the same rainfall event. The first scenario considers the existing land cover while the second one concerns a conversion of the traditional roofs to GRs in respect of the building attributes for GR retrofit. The use of high-resolution satellite imagery from Google Earth has allowed to identify the buildings suitable to host a retrofitted GR. The case study is Preturo municipality in Southern Italy. The city has been selected as located within Sarno river basin which is frequently affected by urban flooding and the massive increase in the occurrence of flash floods mainly took place between 1995 and 2016. It has been shown that, such an increase cannot be directly linked to climate change (Califano et al., 2015) but it could be related to the uncontrolled expansion of soil sealing in the same period. In the last case, the GR retrofit of existing roofs within the considered area could lead to a successful stormwater management. The analysis of the variation of impervious area has been performed using two set of SAR (Synthetic Aperture Radar) images: 1995s images provided by ERS-1 sensor and 2016s images supplied by COSMO-SkyMed sensor. The obtained temporal coherence maps have been treated with the color thresholding method for image segmentation so as to isolate urban pixels and detect the change in time of the paved surfaces.

2 MATERIAL AND METHODS

SWMM model has been used to predict the hydrological response of the drainage network resulting from two GR conversion scenarios within Preturo municipality. The first scenario is the actual one while the second scenario refers to the greening conversion of buildings which meet predefined criteria. The adoption of GRs for the retrofitting of existing roofs in order to mitigate urban flooding events, confirms to be an appropriate solution mainly if within the considered area, a rapid and uncontrolled urbanization has occurred during the studied period. The analysis of land cover change during the last two decades (from 1995 to 2016), has been performed by means of the elaboration of SAR images.

2.1 Case Study

The case study is Preturo municipality in Campania region (Southern Italy). It is a poorly populated and urbanized area with 1768 inhabitants for a surface of

about 28 hectares. The altitude of the municipality is about 190 m above sea level. According to Koppen classification, the site is characterized by Mediterranean climate (Csa) with hot, dry summers and cool, wet winters with the highest percentage of rain in the year. The temperature here averages 15.2° C while the rainfall in a year, is about 845 mm. The city has been selected as all the details concerning its urban drainage system are available and furthermore, it is located within Sarno river basin (Figure 1) which is a risk-prone area where a large number of flooding events occurred during the last decades.

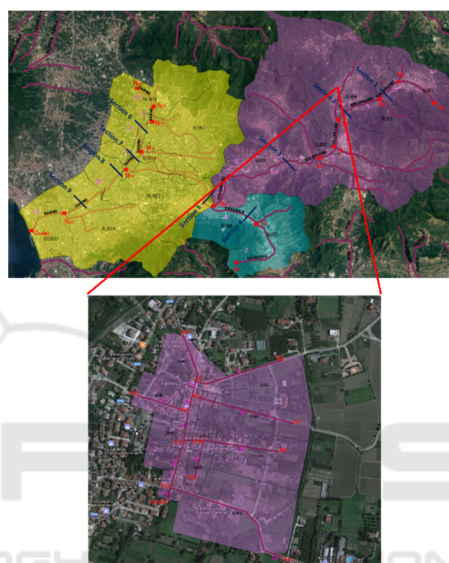


Figure 1: Preturo municipality as part of Sarno basin.

Indeed, during the last two decades, the Sarno river basin has experienced a massive increase in the occurrence of flash floods (Figure 2)

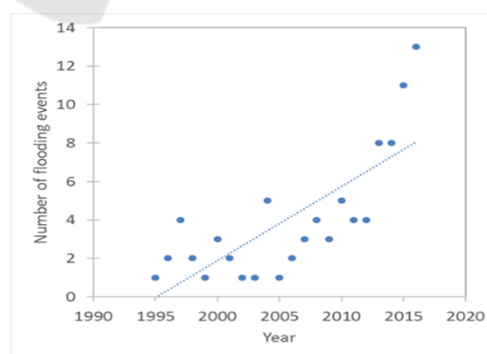


Figure 2: Floods occurred between 1995 and 2016 in Sarno river basin.

It has been argued that, the increase in the frequency of flooding events between 1995 and 2016 in Sarno basin, is not linked to climate change

(Califano et al. 2015) but it could be related to the rapid urbanization of the area during the same period.

If so, the GR retrofit of existing roofs would result the most appropriate choice for urban stormwater management.

2.2 SAR Images Elaboration

Remote sensing imagery has been used to detect the land use/cover change transitions between 1995 and 2016 in the Sarno river basin, in order to identify a correlation between the increase of paved surfaces and of the hydrological damaging events. The process here proposed for the elaboration of SAR images, can be organized in three major blocks (Figure 3).

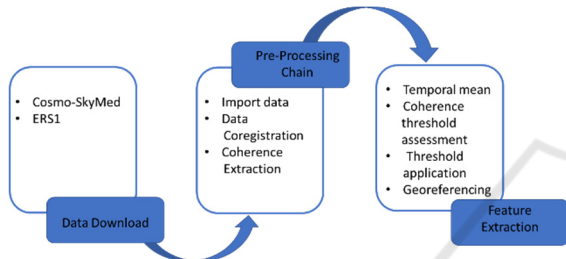


Figure 3: Processing algorithm.

The first step was the data download. Two sets of archive satellite images have been used (Table 1). The first set of images consists of 6 images acquired between March and December 1995 by the ERS-1 satellite and distributed by the European Space Agency (ESA), the second dataset has been acquired by the COSMO-SkyMed sensor between May and December 2016, and consists of 7 images distributed by the Italian Space Agency (ASI).

Table 1: Acquisition date of SAR images.

ERS1	COSMO-SkyMed
Acquisition date	
24th March 1995	3rd May 2016
8th July 1995	20th June 2016
12th August 1995	6th July 2016
21st October 1995	8th September 2016
25th November 1995	24th September 2016
30th December 1995	27th November 2016
-	13th December 2016

The pre-processing block includes data coregistration and the estimation of the interferometric coherence. Coregistration is the process of alignment of the images with the reference one, which is usually the first acquired. In the present

study, the reference images for the ERS1 and COSMO-SkyMed time series have been acquired, respectively, on March 1995 and May 2016.

The pre-processing block also includes the interferometric coherence estimation. It is a measure of the stability of a target with respect to the phase of the complex signal. Considering two co-registered images, it is computed through the following relation:

$$\gamma = \frac{|\sum S_1(x) \cdot S_2^*(x)|}{\sqrt{|\sum |S_1(x)|^2 \cdot |\sum |S_2(x)|^2}} \quad (1)$$

Where S_1 and S_2 are respectively the complex image values for the first and the second image while * represents the complex conjugation operation. The reference image used in this step is the reference image of the coregistration phase. The coherence ranges between 0 and 1 respectively referring to the natural land cover and the built-up area.

The feature extraction block includes the temporal mean of the coherence consisting of averaging per year the multi-temporal SAR images of coherence in order to reduce the speckle but not the spatial resolution. The second activity of the block is the coherence threshold assessment carried out using Otsu's method allowing to convert a grey level image to monochrome (or binary) image where the white pixels represent the impervious surfaces while the black one the previous ones according to the following equation:

$$\sigma_w^2(t) = W_b(t) \cdot \sigma_b^2(t) + W_f(t) \cdot \sigma_f^2(t) \quad (2)$$

The best threshold value t^* corresponds to the minimum within class variance σ_w . W_b and W_f are the weights of the foreground and background classes of pixels given as:

$$W_b(t) = \sum_{i=1}^t P(i); \quad W_f(t) = \sum_{i=t+1}^I P(i) \quad (3)$$

Where:

$$P(i) = \frac{n_i}{n} \quad (4)$$

The symbol i represents the gray-level and n_i the quantity of the pixels with the specified gray-level, n is the general number of pixels in the image, I is the maximum pixel value. σ_f^2 and σ_b^2 are the variances of the two classes:

$$\sigma_b^2 = \frac{\sum_{i=1}^t (i - \mu_b(t))^2 \cdot P(i)}{W_b(t)} \quad \text{with} \quad \mu_b = \sum_{i=1}^t \frac{i \cdot P(i)}{W_b(t)} \quad (5)$$

$$\sigma_f^2 = \frac{\sum_{i=t+1}^I (i - \mu_f(t))^2 \cdot P(i)}{W_f(t)} \quad \text{with} \quad \mu_f = \sum_{i=t+1}^I \frac{i \cdot P(i)}{W_f(t)} \quad (6)$$

Where μ_f and μ_b are the mean of the two classes.

Finally, the processing of the two sets of satellite images from ERS-1 and COSMO-SkyMed sensors has allowed to detect the variation in the sealing surfaces during the considered period and to find a possible correlation between it and the increasing occurrence of hazardous events within the studied area. If a link exists the implementation of green infrastructures, with the aim of reducing the risk associated to severe events in urban area, can be investigated. The implementation of these infrastructures is closely related to the potential for retrofitting of existing roofs investigated as explained in the following chapters.

2.3 Building Attributes for Green Roofs

The hydrologic effect of two GR conversion scenarios, at the city scale, has been tested using SWMM. The first scenario considers the existing land cover where no GRs are installed while the second one benefits from the greening conversion of some traditional roofs of the city. Sustainability for GR retrofit has been detected using Google Earth and it mainly depends on four criteria (Wilkinson and Reed, 2009) that are:

- Roof slope;

The greening should be applied to roof with a minimum slope of 2% and a maximum slope of 45%.

Roofs with a slope less than 2% require additional drainage measures in order to avoid waterlogging in the vegetation support course. On the other hand, a sloped roof retains less water and structural and vegetation problems could occur like the slip of the plant layer.

- Number of stories;

Taller buildings could partially or totally overshadow the adjacent smaller ones and the shadow could affect negatively the grow of the plants and reduces evapotranspiration fluxes. Because the height of each building is unknown, the number of stories has allowed to discern the taller and the smaller buildings.

- Orientation of the roof;

In general, the sunlight contributes to the welfare of the vegetation and in the northern hemisphere, the exposure to direct sun is higher for south-facing buildings.

- Number of site boundaries;

If a building is attached to others on four sides, during the construction of GR, the access for machinery and delivery or storage of materials tend to be difficult just like the subsequent access for maintenance. In view of this, the buildings bounded on four sides should be discarded.

2.4 Model Overview, Setup and Implementation

The EPA Storm Water Management Model (SWMM) has been selected as the approach for studying the runoff production in both the considered scenarios. SWMM is a dynamic hydrology-hydraulic simulation model originally developed for urban areas. SWMM consists of several blocks for analysis of different processes: the Runoff block which performs hydrologic simulation of runoff production, the Transport and Extended Transport block for the routing of this runoff, the Storage/Treatment block which characterizes the effects of control devices upon flow and quality and elementary cost computations and the receive block which considers the mix of the produced runoff in a receiving water body. SWMM is equipped with a LID module used to model various stormwater management devices including GRs. SWMM solves the complete form of Saint-Venant equations over the drainage network. The Saint-Venant equations for conservation of mass and momentum can be respectively express as follows:

$$\delta Q / \delta t + \delta A / \delta x = 0 \quad (7)$$

$$\frac{\delta Q}{\delta t} + \frac{\delta(Q^2/A)}{\delta x} + gA \frac{\delta H}{\delta x} + gAS_f + gAh_L = 0 \quad (8)$$

where A is the cross-sectional area, t is the time, Q is flow rate, x is distance, H is hydraulic head of water in the conduit, g is the gravity, h_L represents the local energy loss per unit length of conduit; and S_f is the friction slope. SWMM solves the Saint-Venant equations using an explicit finite difference method and successive approximation. The continuity equation (Eq. 7) states that in any control volume of water, the net change of mass caused by the inflow and outflow equals the net rate of change of mass in the same control volume. The momentum equation (Eq. 8) asserts that the rate of change of momentum in the control volume of water equals all the external forces acting on the same control volume. Preturo's sewer network including the junction nodes, the twelve sub-catchments (from SUB1 to SUB12), the conduits can be sketched in SWMM as in Figure 4a. The model has run with a rainfall input referring to the event occurred on 13/09/2012 and recorded by the local rain gauge. The rainfall event has been selected as it caused severe flash flood in the considered area. It lasted about 17 hours with a cumulative rainfall of 56.4 mm and a return period of 8 years. The temporal distribution of the event is shown in Figure 4b.

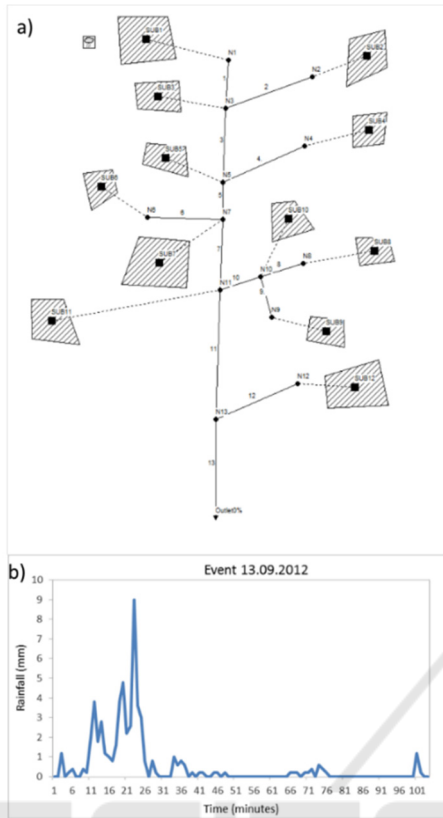


Figure 4: a) Urban drainage system of Preturo in SWMM, b) Rainfall input.

The GR used for the simulation is an experimental roof located in the campus of university of Salerno. It is of extensive type and it is made up of three layers for a total thickness of 15 cm: the vegetation layer where the plants grow, 10 cm deep support substrate which ensures a suitable growing environment for the vegetation, and a water storage layer of 5 cm where the water can be retained.

The support layer is mainly composed of peat while the storage layer is made up of expanded clay (Figure 5).

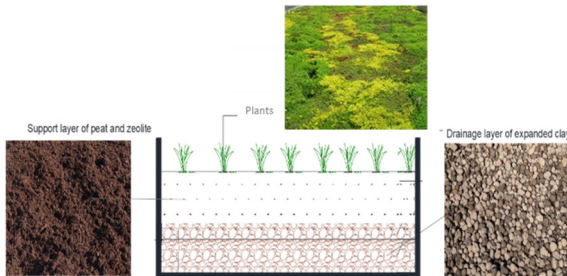


Figure 5: GR structure.

More details about the characteristics of the considered GR and the input parameter set of the GR module used for running the model are available in (Mobilia, 2018).

Due to the lack of flow measurements within the basin, the calibration procedure of the model has not been performed, anyway, since several rainfall/runoff events have been recorded at the experimental roof, the calibration of the LID module has been carried out instead. For more details about the observed events, the calibration procedure and parameters please consult Mobilia and Longobardi (2020c) and Mobilia et al. (2020).

2.5 The Performance Analysis

The event-based performance is assessed through three indices: the percentage of reduction in runoff volume (ΔRV), in peak flow (ΔPF) and increase in the delay time (ΔDT). The indices have been estimated as follows:

$$\Delta R_V = \frac{R_{V,0} - R_{V,1}}{R_{V,0}} \cdot 100 \quad (9)$$

$$\Delta P_F = \frac{P_{F,0} - P_{F,1}}{P_{F,0}} \cdot 100 \quad (10)$$

$$\Delta D_T = \frac{D_{T,0} - D_{T,1}}{D_{T,0}} \cdot 100 \quad (11)$$

Where $R_{V,0}$, $P_{F,0}$, $D_{T,0}$ are respectively the runoff volume (m^3), the peak flow (m) and the delay time (min) referred to the baseline scenario, while $R_{V,1}$, $P_{F,1}$, $D_{T,1}$ are the same parameters but referred to the greening scenario. The indices have been calculated with respect to the outlet sections of each sub-catchment and of the whole basin.

3 RESULTS

Remote sensing imagery has been used to detect the land use/cover change transitions between 1995 and 2016 in the Sarno river basin. The results of SAR images elaboration show that the build-up area moved from about 7% to about 12% between 1995 and 2016, so Sarno watershed has experienced a rapid urbanization during the last two decades (Figure 6). This finding suggests that the increase in the occurrence of flooding events within Sarno basin could be attributable to the overbuilding of the surface, therefore, the retrofitting of buildings with

GRs may represent a valid solution to mitigate the negative effects of hydrological damaging events.

The hypothesis that GRs, applied at large scale, could be effective in managing the urban stormwater management in an overbuilding area, is hereinafter tested with the use of SWMM.

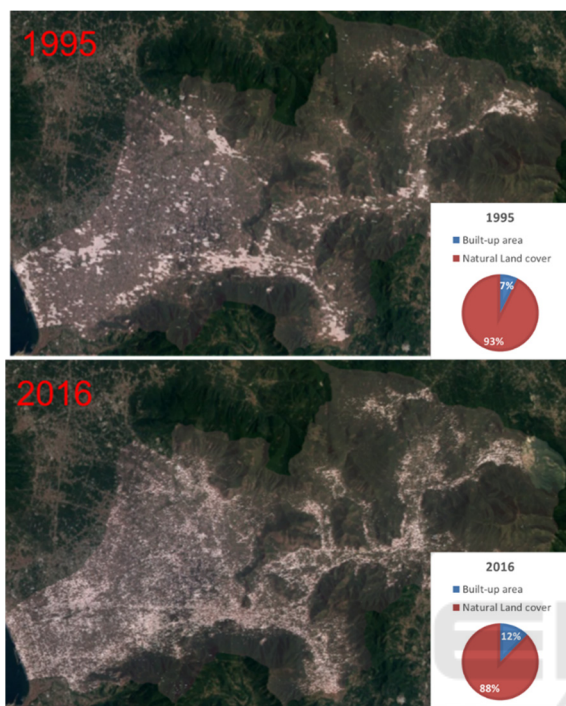


Figure 6: The change in built-up area between 1995 and 2016.

The hydrological behavior of the drainage network in two scenarios has been analyzed. The first scenario is the baseline one while the second scenario involves the widespread GR implementation within the area according to four factors affecting the potential to retrofit existing roofs which are: roof slope, number of stories, orientation of the roof, number of site boundaries. The identification of the suitable buildings has been visually performed by means of the images provided by Google Earth. With respect of the roof slope, all the existing buildings meet the requirement. As regards the criteria of number of stories, the buildings with such a height as not to be overshadowed by the nearby ones represents the 7.1% of the total area of the basin (Figure 7). In particular, the average number of stories is two. Overall, 24 buildings are one story, 80 are two stories and 72 are three stories. Only 1% of the total buildings are four stories buildings.

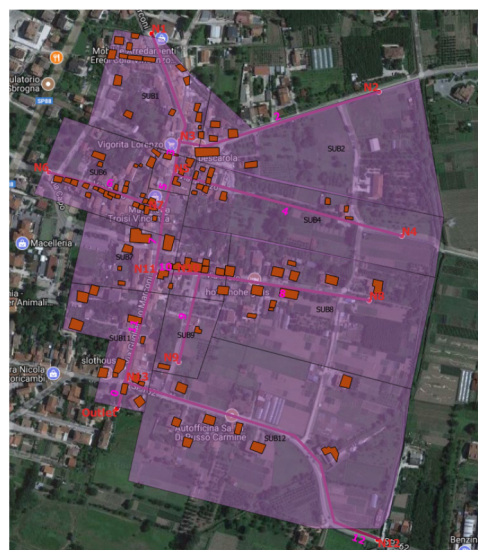


Figure 7: Buildings selected according to the number of stories.

The examination of site orientation revealed that the south-facing buildings are about 10% of the total basin area (Figure 8).

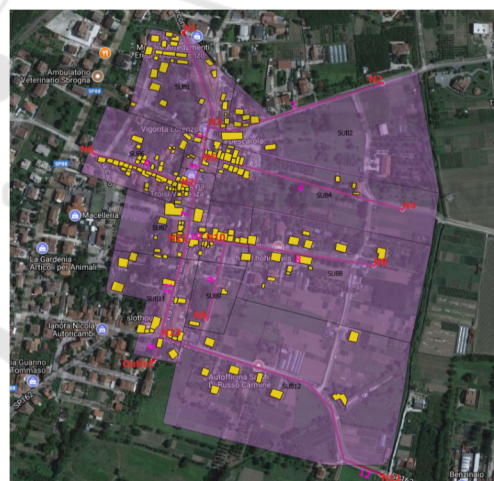


Figure 8: Buildings selected according to the orientation of the existing roofs.

With references to criteria of number of site boundaries (Figure 9) which aims at discarding the buildings bounded on four sides, it can be said that most of houses have not neighboring buildings (29% of the total houses) so are free-standing while the 23% of the buildings are bounded on two sides and the 21% on three sides. Only 15% of the total buildings are bounded on one side. In conclusion, the buildings which comply with this criteria represent the 9% of the total basin area. Finally, the buildings which meet all the attributes required for GR adaptation occupied

on average about the 7% of the area of the whole basin. This percentage has been used to reproduce, in SWMM, the hydrological behavior of a hypothetical greening scenario which has been subsequently compared to the baseline scenario where the existing land cover of the basin is considered.

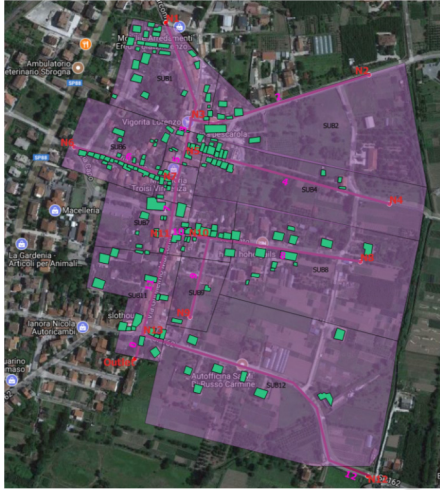


Figure 9: Buildings selected according to the number of site boundaries.

The comparison has been performed in terms of produced runoff volume, peak flow and delay time. At a first visual inspection of the runoff hydrographs observed at the outlet section of the whole basin (Figure 10), it is possible to observe how, the runoff volume and the peak flow are visibly lower in the case of the GR retrofit scenario than for the baseline one.

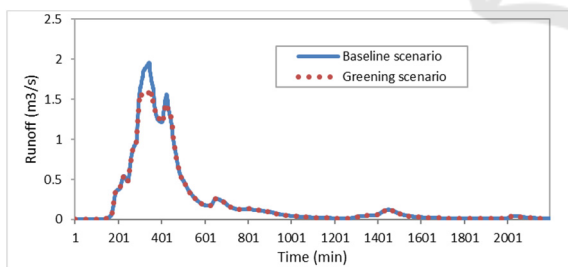


Figure 10: Comparison of existing land use condition hydrograph with the greening conversion hydrograph at the catchment outlet.

For a comparison in quantitative terms, the assessment of three indices whose values are shown in Table 2, has been performed. A reduction of the runoff volume and of the peak flow of respectively 3.8% and 18.9% has been detected for the whole basin after the GR conversion of the existing buildings while an increase of the delay time of 8.2% can be observed. At the single sub-catchment scale,

after the GR retrofit, the runoff reduction ranges from the minimum value of 0.8% to the maximum value of 9.4%. The GR performances in terms of peak flow reduction and delay time increase are lower if compared to the ones obtained for the whole basin indeed, they reach respectively at most the 3.6% and 0.8%. The worst performances are found in the eastern part of the basin (SUBs 2, 4, 8, 9, 12) where the retrofitting potential is lower.

Table 2: Values of the indices.

Sub	ΔRv (%)	ΔPf (%)	ΔDt (%)
1	5.1	2.6	0
2	1.1	0.0	0
3	8.4	1.6	0.8
4	0.9	0.0	0
5	5.6	1.0	0
6	5.3	1.2	0
7	6.2	1.8	0
8	1.9	0.0	0
9	1.2	0.0	0
10	9.4	3.2	0
11	7.2	3.6	0
12	0.8	0.0	0
Whole	3.8	18.9	8.2

4 CONCLUSIONS

The GR technology is a valid solution to mitigate the risk of flooding in urban areas especially in the territory interested by a rapid and uncontrolled soil sealing. This is the case of the Sarno river basin that between 1995 and 2016, has experienced a doubling of the build-up area. The aim of this research is to investigate and compare the hydrological performance of two scenarios respectively with and without the adoption of GRs for the retrofitting of existing roofs in Preturo municipality which is part of Sarno river basin. The factors impacting the potential for the retrofit of an existing roof are the number of stories, the orientation of the roof, the number of site boundaries and the roof slope which have been verified with Google Earth. The percentage of GR retrofit potential in the basin is 7% of the total area. The analysis has been performed using SWMM and showed that the widespread GR implementation at the

whole basin scale reduces the peak runoff rates and the runoff volumes respectively by up to 4% and 19 % while it increases the delay time of about 8%. In conclusion, in poorly urbanized area, the application of GRs at large scale, returns a good attenuation of flooding events but the technology could be better performing in densely populated areas. For higher attenuation of the urban floods, the GR infrastructures could be used in combination with different types of LID practices. Future research directions of the present work are twofold. From one side, the building selection can be improved by using geospatial data such as Lidar and photogrammetry mapping technologies. From the other side, the identification of the pervious/impervious surfaces can be optimized by combining SAR and optical images. The joint use of the both types of images allows to overcome the limitations of the two approaches. Indeed, the optical images have a high spatial resolution but suffer from the problem of the cloud cover and vice versa for SAR images.

REFERENCES

- Califano, F., Mobilia, M., Longobardi, A., 2015. Heavy Rainfall Temporal Characterization in the Peri-Urban Solofrana River Basin, Southern Italy. *Procedia Engineering*, 119, 1129-1138.
- Chui, T. F. M., Liu, X., Zhan, W., 2016. Assessing cost-effectiveness of specific LID practice designs in response to large storm events, *Journal of Hydrology*, 533, 353-364.
- Haowen, X., Yawen, W., Luping, W., Weilin, L., Wenqi, Z., Hong, Z., Yan Yichen, Jun, L., 2020. Comparing simulations of green roof hydrological processes by SWMM and HYDRUS-1D, *Water Supply*, 20(1), 130-139.
- Khramtsova, L., Leonteva, M., Mobilia, M., Longobardi A., Nasyrova, E., Aksenov, S., 2020. Characterization of rainfall events corresponding to forecasted conditions of potential hydrogeological risk, *Journal of Physics: Conference Series*, 1614(1),012077.
- Krasnogorskaya, N., Longobardi, A., Mobilia, M., Khasanova, L. F., Shchelchkova, A. I., 2019. Hydrological modeling of green roofs runoff by Nash cascade model, *The Open Civil Engineering Journal*, 13(1), 163-171
- Longobardi, A., D'Ambrosio, R., Mobilia, M., 2019. Predicting stormwater retention capacity of green roofs: An experimental study of the roles of climate, substrate soil moisture, and drainage layer properties, *Sustainability*, 11(24), 6956.
- Longobardi, A., Diodato, N., Mobilia, M., 2016. Historical storminess and hydro-geological hazard temporal evolution in the solofrana river basin—Southern Italy, *Water*, 8(9), 398.
- Mobilia, M., 2018. Sustainable management of stormwater in a changing environment under Mediterranean climate conditions, *PH.D. dissertation*.
- Mobilia, M., Califano, F., Longobardi, A., 2015. Analysis of rainfall events driving MDHEs occurred in the Solofrana River Basin, Southern Italy, *Procedia Engineering*, 119, 1139-1146.
- Mobilia, M., D'Ambrosio, R., Longobardi, A., 2020. Climate, soil moisture and drainage layer properties impact on green roofs in a Mediterranean environment. *In Frontiers in Water-Energy-Nexus—Nature-Based Solutions, Advanced Technologies and Best Practices for Environmental Sustainability*. Springer, Cham.
- Mobilia, M., Longobardi, A., 2017. Smart stormwater management in urban areas by roofs greening. In *ICCSA2019, International Conference on Computational Science and Its Applications*. Springer, Cham.
- Mobilia, M., Longobardi, A., 2020a. Model Details, Parametrization, and Accuracy in Daily Scale Green Roof Hydrological Conceptual Simulation. *Atmosphere*, 11(6), 575.
- Mobilia, M., Longobardi, A., 2020b. Impact of rainfall properties on the performance of hydrological models for green roofs simulation. *Water Science and Technology*, 81(7), 1375-1387.
- Mobilia, M., Longobardi, A., 2020c. Event scale modeling of experimental green roofs runoff in a mediterranean environment. *In Frontiers in Water-Energy-Nexus—Nature-Based Solutions, Advanced Technologies and Best Practices for Environmental Sustainability*. Springer, Cham.
- Mobilia, M., Longobardi, A., Sartor, J. F., 2017. Including a-priori assessment of actual evapotranspiration for green roof daily scale hydrological modelling. *Water*, 9(2), 72.
- Sartor, J., Mobilia, M., Longobardi, A., 2018. Results and findings from 15 years of sustainable urban storm water management. *International Journal of Safety and Security Engineering*, 8(4), 505-514.
- Starry, O., Lea-Cox, J., Ristvey, A., Cohan, S., 2016. Parameterizing a water-balance model for predicting stormwater runoff from green roofs, *Journal of Hydrologic Engineering*, 21(12), 04016046.
- Versini, P. A., Ramier, D., Berthier, E., De Gouvello, B., 2015. Assessment of the hydrological impacts of green roof: From building scale to basin scale. *Journal of Hydrology*, 524, 562-575.
- Wanniarachchi, S. S., Wijesekera, N. T. S., 2012. Using SWMM as a tool for floodplain management in ungauged urban watershed, *Engineer: Journal of the Institution of Engineers, Sri Lanka*, 45(1). 1-8
- Wilkinson, S.J., Reed, R., 2009. Green roof retrofit potential in the central business district. *Property Management*, 27(5), 284-301.